Modelling of Unconfined Flame Tilt in Cross-Winds

Yasushi OKA
Department of Safety Engineering, Yokohama National University
79-5 Tokiwadai, Hodogaya-ku, Yokohama 240-8501, Japan

Hitoshi KURIOKA and Hiroomi SATOH
Kajima Technical Research Institute
19-1 Tobitakyu 2 Chome, Chofu-shi, Tokyo 182-0026, Japan

Osami SUGAWA
Center for Fire Science and Technology, Science University of Tokyo
2641 Yamasaki, Noda 278-8510, Japan

ABSTRACT

Experiments were conducted to characterize the effects of cross-wind on flame properties for unconfined fires. Propane gas was used as a fuel in a 0.1m×0.1m diffusion burner employed as a model fire source. The effects of the floor around a fire source, which would control the volume of air entrained into the hot current, were also investigated. Empirical models of the apparent flame height of the inclined flame are presented. We also develop empirical models of the flame tilt angle based on the balance of mass fluxes given by the upward hot current and cross-wind. These models are based on functions of dimensionless heat release rate and Froude number. The values of empirical coefficients and exponents were derived from the experimental results. The calculated flame length based on the flame tilt angle and the apparent flame height was compared with experimental results, showing that models can be used to estimate flame length in cross-winds.

KEYWORDS : unconfined fire, cross-winds, flame tilt, apparent flame height, flame length

NOTATION LISTS

A, B : coefficient
D : reference length of fire source (m)
g : acceleration due to gravity (m/sec^2)
H : effective height (m)
H_f : vertical length from the intersection of the isotherm curve of 250℃ and the flame axis to burner surface level (apparent flame length)
L_{ft} : length along the flame axis from the centre of the burner surface to the intersection of the flame axis and the isotherm curve of 250℃
L_{fw} : length of the straight line from the centre of the burner surface to the intersection of the flame axis and the isotherm curve of 250℃

T_o : ambient temperature (℃)
U_{wind} : representative wind velocity (m/sec)
W : effective width (m)
W_o : upward velocity at centerline of the plume (m/sec)
X_1 : horizontal length from the intersection created by the extrapolated plume axis to the centre of the burner surface
X_2 : horizontal length from the intersection of the isotherm curve of 250℃ and the flame axis to the centre of the burner
z : height from the burner surface (m)
ρ_o : wind density (kg/m3)
F_b : buoyancy force (kg·m/sec2)
F_i : inertia force (kg·m/sec2)
$\dot{M}_b$: mass flux of hot current (kg/sec)
$\dot{M}_i$: mass flux of wind (kg/sec)
Fr_{wind} : Froude number $(=U_{wind}^2 / gD)$
Q^* : dimensionless heat release rate $(=Q/\rho_o C_p T_o g^{1/2} D^{5/2})$
θ_1 : the angle created by the intersection of the floor level and extrapolated plume axis.
θ_2 : the angle formed by the straight line between the centre of the burner surface and the intersection of the flame axis and the front of the isotherm curve of 250℃.

INTRODUCTION

The practical importance of flame tilt, i.e. on flame spread, could usefully be mentioned. Flame heights are simply related to Q^* regardless of the shape of fire sources and their sizes [1-5]. Although many studies of flame tilt have been reported and several models derived for estimating the flame tilt angle of tank fires or urban fires [6-14], few papers have reported the basic information about heat release rate employed and the position at which a representative wind speed is defined.

We could estimate the upward velocity along the flame/plume axis with the aid of knowledge of fire physics in calm conditions, but it is difficult to predict the vertical velocity component of a hot current along the inclined trajectory as affected by cross-winds. It is also extremely difficult to quantify the local wind field close to a fire source.

It is therefore proposed that, when estimating the flame tilt angle, a more realistic method is for heat release rate and representative wind velocity to be used as substitute variables for upward and wind velocities respectively. A new approach is thus presented, in which the apparent flame height acts as an additional function to allow the effects of cross-winds on flame tilt to be readily encompassed.

MODELING OF FLAME TILT ANGLE

In this study the flaming region is defined by temperature instead of a visual record. Hence the accuracy of the tilt angle depends strongly on the temperature of the isotherm used to delineate the flame. Figure 1 (a), (b) shows a comparison between flaming regions given by a 35mm camera and isotherm curves. The flaming region given by a 35mm camera corresponds approximately to the ΔT =200～250℃ isotherm. Thus ΔT =250℃ is employed to define the flaming region. Selection of this temperature rise is supported by the literature [1].

Since the unconfined flame length in the absence of a cross-wind can be described as a function of the heat release rate and fire size, the inclined flame length in the presence of a cross-wind may also be approximated as a function of the heat release rate and the representative wind velocity, represented in dimensionless form as follows.

$$L_{fw} / D = f(Fr_{wind}, Q^*) \qquad (1)$$

It is, however, difficult to define the flame length as affected by wind, because this length can be obtained by several means. For example, the length can be simply defined from the tip of the flame to the centre of the fire source, or, along the flame axis from the centre of fire source to the flame tip whose locus then becomes an arc. In analogy to equation (1), the apparent flame height of an inclined flame may also be represented as follows, equation (2).

$$H_f / D \propto L_{fw} / U_{wind}^2 \propto Fr^m \cdot Q^{*n} \qquad (2)$$

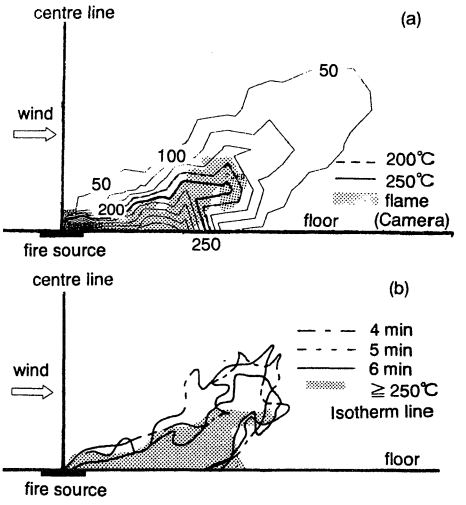

Figure 1 Comparison of the flaming region given by a 35mm camera and isotherm curve of 250 ℃. Q=8.0kW, V=2.0m/sec
(a) Flaming region is plotted on the isothermal curves. (b) Flames caught by a 35mm camera at several times super-imposed on the isothermal curve of 250℃.

Use of this length leads to a simple definition and avoids the necessity for inconvenient measurements. Furthermore, we consider that it is more useful to employ the apparent flame height and vertical rise of the axis of the flame when estimating the thermal intensity in the vicinity of the fire source.

As a starting point, mass fluxes representing the upward hot current and wind were employed considered to be the main factors in determining the tilt angle. These are combined with the centerline properties based on upward velocities in calm conditions, by assuming that the centerline properties are succeeded under the presence of a cross-wind. We also bring the two kinds of height into the model, namely practical flame height and architectural spatial height to represent the flame tilt behaviour.

The flame tilt angle is assumed to be controlled by the balance of mass fluxes of the hot current and cross-wind at the average flame height. The mass flux of the cross-wind becomes

$$\dot{M}_i \propto \rho_o U_{wind} D H_f \qquad (3)$$

The mass fluxes in the intermittent and/or plume region can be described by employing the relations for the upward velocity along the centerline as proposed by McCaffrey,

$$\dot{M}_b \propto \pi\rho_o Q^{1/5} z^2 \quad \text{(for intermittent region)} \quad (4)$$

$$\dot{M}_b \propto \pi\rho_o (Q/z)^{1/3} W_o z^2 \propto \pi\rho_o Q^{1/3} z^{5/3} \quad \text{(for plume region)} \quad (5)$$

Combining Equations (3) - (5), we obtain two alternative models for flame tilt angle;

$$\text{Model 1} \quad \tan\theta = \frac{\dot{M}_i}{\dot{M}_b} \propto \frac{Fr_{wind}^{1/2}}{Q^{*1/5}} \cdot \frac{D}{H_f} \quad \text{(for intermittent region)} \quad (6)$$

$$\text{Model 2} \quad \tan\theta = \frac{\dot{M}_i}{\dot{M}_b} \propto \frac{Fr_{wind}^{1/2}}{Q^{*1/3}} \left(\frac{D}{H_f}\right)^{2/3} \quad \text{(for plume region)} \quad (7)$$

It is possible to obtain alternative models by considering a balance of the inertial force of the cross-wind and the buoyancy force of the hot current used to determine the angle of the inclined flame [16].

DEFINITION OF THE FLAME TILT AND THE FLAME LENGTH

The upward velocity close to the fire source has relatively weak buoyancy compared to potential of cross-winds and the flame is pushed downstream, sometimes showing a spread at the base of the flame. The upward velocity, however, gradually increases as buoyancy increases with height and the flames tend to rise vertically.

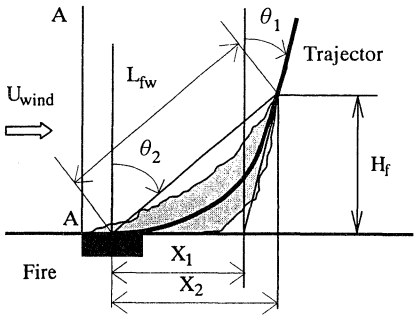

Figure 2 Definition of angle and several lengths.

This paper focuses on the unconfined flame tilt, but ideally we would also aim to apply this model to confined spaces such as a tunnel or a corridor under forced ventilation, and hence improve the accuracy with thermal intensity is estimated in the near field of a fire source. If, depending on the heat release rate, height of the confined space and the ventilation rate, we assume that flames impinge on the ceiling, then, it is meaningless to define the tilt angle via the means of flame defined between the tip of the flame to the centre of the fire source. This angle would correspond to θ_2. Hence, we define another flame tilt angle, θ_1, shown in Figure 2 defined using length X_1. Both these tilt angles are measured from the vertical.

EXPERIMENTAL PROCEDURE

Figure 3 shows a schematic diagram of the experimental apparatus. The burner, ventilation duct and a false floor (0.6m wide and 1.6m long) are set 0.9m above the floor of the experimental facility. Reference to "with floor" refer to the situation when the burner surface,

the bottom of the duct and the false floor are at the same level and "without floor" when the false floor is absent. Reference to "with floor" assume to the situation of a spill of flammable liquid and "without floor" to a tank fire.

The porous gas burner, of dimension 0.1m × 0.1m, was positioned at a distance of 1.2m from the ventilation duct. Propane gas was used as a fuel. The heat release rate was varied in the range of 0.75 to 16 kW. This heat release rate corresponds to pool fires ranging from 0.2 to 4.5 for Q^*.

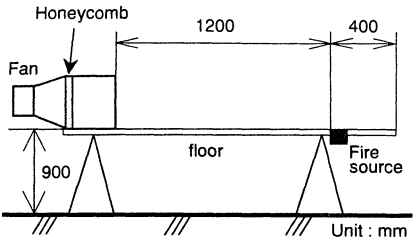

Figure 3 Schematic diagram of experimental set up

A cross-wind was supplied from the rectangular duct, whose dimensions are 0.3m×0.3m, connected to the fan via a honeycomb filter. The flow rate was varied in the range of 0.5 to 4.0 m/sec. These values correspond to value of 0.18 to 12.5 for Fr_{wind} at the section AA' in Figure 2.

The temperature field was measured using K-type thermocouples with a diameter of 0.65 mm. Thermocouples arranged to cover a downward region of 0.9m(W)×0.9m(H), a total of 143 points, with the datum set at the centre of the burner. Isotherm curves were constructed using these temperatures. Values for temperature were taken from average over the last 3 minutes, one of a 10 minute test, this duration being assumed to be at a quasi steady state for both heat release rate and cross-wind velocity.

RESULTS AND DISCUSSIONS

Wind velocity and flame angle

Typical vertical wind profiles at cross section AA' in Figure 2 are shown in Figure 4. The main region of interest is up to 30cm above the level of the false floor. The profiles are clearly affected by the development of the boundary layer in the presence of the false floor. Moreover, the velocities at more than 30cm above the level of the false floor drop to less than 50% of the maximum velocity. This vertical profile is assumed to be characteristic of the horizontal profile

Only data in which the apparent flame height is less than 30cm is used in this work. We also employed a representative mean velocity, by dividing the total volumetric flow by the

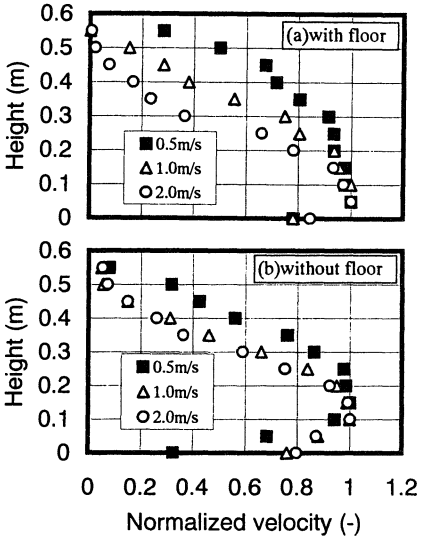

Figure 4 Typical vertical wind profile at cross-section AA' in the absence of a flame.

effective height and width, as shown in equation (8).

$$\bar{v} = \iint v_i(h)dhdw/(H \cdot W) \tag{8}$$

Comparison of θ_1 and θ_2

Figure 5 shows the comparison between θ_1 and θ_2. In the case of "without floor", the difference between θ_1 and θ_2 is small and they show almost the same angle. In the case of "with floor", the angle defined by θ_2 is greater than θ_1. Flames show large tilt angle under the condition that Q^* is small and Fr_{wind} is large.

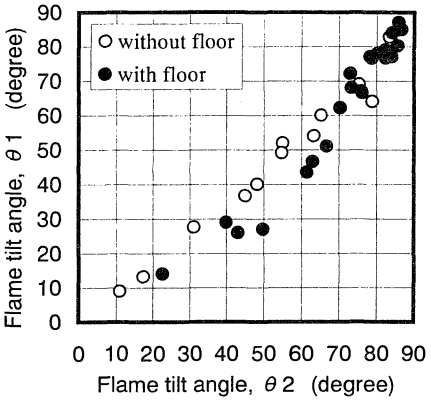

Figure 5 Relationship between θ_1 and θ_2.

Apparent flame height

We observed that the apparent flame heights in the presence of a cross-wind are shorter than those in its absence, regardless of the existence of the false floor or not, illustrated in Figure 6. It is considered that the fresh air entrained into the combustion region enhances the combustion efficiency and the cooling effect of the cross-wind. Secondly, the apparent flame height of "with floor" is shorter than that of "without floor" for the same heat release rate and wind velocity. This result means that the flames in the presence of the false floor tend to have a large angle of inclination than those in the absence of a floor. These results are probably due to the differences in entrainment of surrounding air into the flaming region.

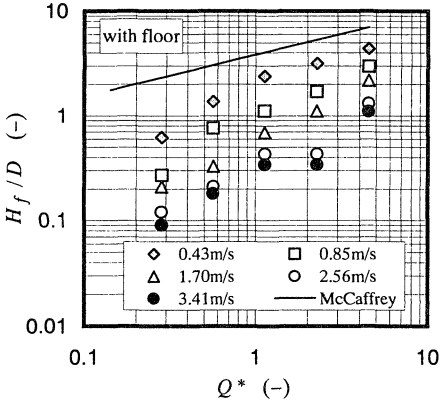

Figure 6 Variation of apparent flame height against Q^* in the case of "with floor".

Figure 7(a), (b) shows the relation between the apparent flame height and the function of Fr_{wind} and Q^*. The data can be matched closely by the following expression, equation (9).

$$\frac{H_f}{D} = \alpha\left(\frac{Fr_{wind}^n}{Q^*}\right)^{-3/4} \tag{9}$$

- with floor (the surface of fire source is positioned at the same level as the floor)

  α =0.88, n=2/3, $0.2 \le Fr_{wind}^{2/3}/Q^* \le 20$

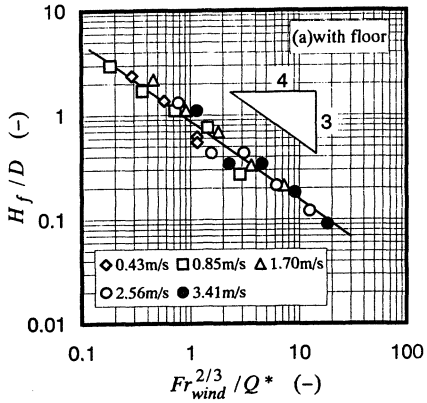

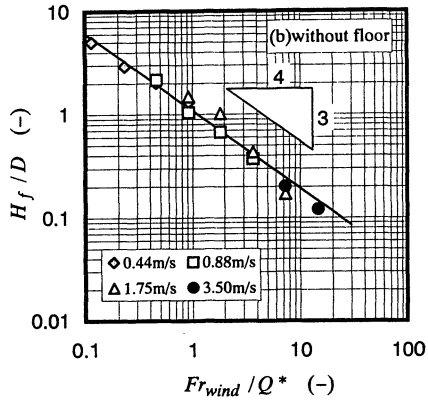

Figure 7 Variation of apparent flame height against Fr_{wind} and Q^*.

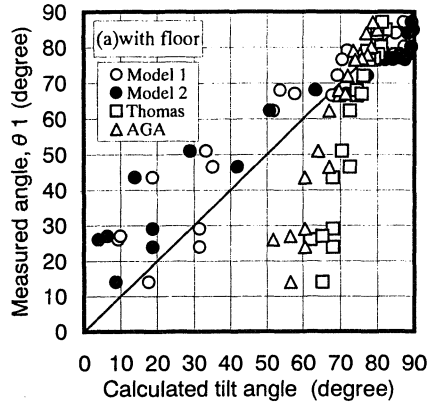

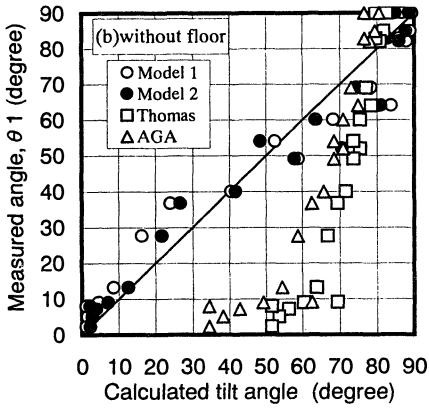

Figure 8 Comparison between predicted and measured tilt angle defined as θ_1 using the coefficient to be unity.

- without floor

  α =1.09, n=1, $0.1 \le Fr_{wind} / Q^* \le 15$

The dependence of Fr_{wind} on the apparent flame height is different according to the local geometry of the fire source. This means that the apparent flame height is strongly affected by the existence of the floor and the value of the power of Fr_{wind} varies from 2/3 to 1, depending on the position of the fire source with respect to the floor. There is a possibility for explanation on dependence of Fr_{wind} that flames move in three-dimensional direction in the absence of a floor, but they only do in two-dimensional direction in the presence of a floor. However the slope of the line shows the same value regardless of the existence of the floor or not. This means that the form of the function for the apparent flame height applies in both cases.

Flame tilt angle

Substituting the models for apparent flame height into equations (6) and (7), considering conditions with and without a floor, allows the values of power to be decided. Figure 8 shows a comparison between predicted and measured tilt angles defined by θ_1, using the coefficient assumed to be of unity. The same behaviour was confirmed for θ_2 [16]. If we consider fires occurring in architectural spaces, there is usually a floor present and then the angle defined by θ_1 becomes the more useful parameter. The results obtained by Thomas and the AGA models are also plotted. As a term for mass loss rate is incorporated in the Thomas and AGA models, the equations were re-written to use flow rate of propane gases instead of the mass loss rate. The tilt angles calculated by the Thomas or AGA models show a tendency to larger tilt angles than experimental results, under conditions of the same heat release rate and wind velocity, regardless of the existence of a floor or not. It is considered that this difference derives from the definition of tilt angle, representative wind and the exact experimental conditions. Thomas model was derived from data using a crib fire source, which has a defined volume. However, our fire is based on an area source. Clearly we have to pay an attention to the experimental conditions for which the model is derived prior to its use.

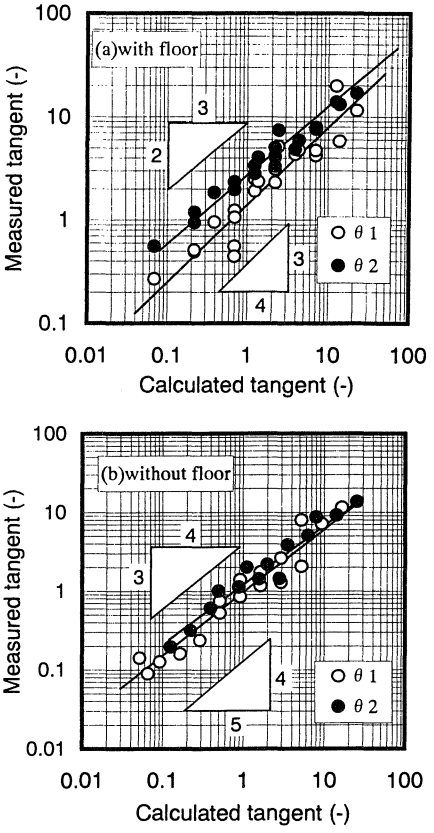

Figure 9 Comparison between predicted and measured tilt angle.

We decided to adopt Model 2, based on statistical measures expressing correlation with experimental data. This model is based on mass fluxes in the plume region.

The scale of spatial and/or time duration from initiation of reaction to termination of reaction essentially controls several commonly observed phenomena, for instance flame expansion at a corner or beside a wall. However, it is very hard to directly incorporate these scales into the present models. We thus adopt a geometrical scale instead of an ill-defined chemical reaction scale to simply describe physical phenomena such as a flame tilt. We tried to represent these differing scales by the spatial scale expanded to the n-th order, with the values of power and coefficient decided with the aid of the relation between measured tilt angle and the calculated one, as shown in Figure 9. Final formula for flame tilt angle are given in equations (10) – (13).

- with floor (the surface of fire source is set at the same level as the floor)

$$\tan\theta_1 = 1.40\left(Fr_{wind}^{5/8}\cdot Q^{*-5/8}\right) \approx 1.40\left(Fr_{wind}^{2/3}\cdot Q^{*-2/3}\right) \quad 30^\circ \le \theta_1 \tag{10}$$

$$\tan\theta_2 = 2.72\left(Fr_{wind}^{5/9}\cdot Q^{*-5/9}\right) \approx 2.72\left(Fr_{wind}^{1/2}\cdot Q^{*-1/2}\right) \quad 40^\circ \le \theta_2 \tag{11}$$

- without floor

$$\tan\theta_1 = 0.96\left(Fr_{wind}^{2/3}\cdot Q^{*-2/3}\right) \tag{12}$$

$$\tan\theta_2 = 1.20\left(Fr_{wind}^{3/4}\cdot Q^{*-5/8}\right) \approx 1.20\left(Fr_{wind}^{3/4}\cdot Q^{*-2/3}\right) \tag{13}$$

In the case of "with floor", equations (10) and (11) are applicable for the range as described above. Equations (12) and (13) also apply to the "with floor" case for the rest of angle.

Final results obtained using equations (10) - (13) are plotted in Figure 10. The models may be applied over a wide range as assured in this study, and it may be considered that this range covers the practical range.

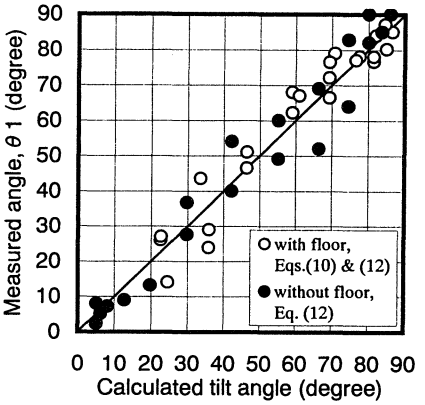

Figure 10 Comparison of calculated and measured tilt angle.

Modelling the intersection defined by θ_1

If we use the relation given by θ_2 and X_2, a series of flame properties, such as tilt angle and flame length, can be deduced. The remaining problem is how to represent the distance X_1. We investigated the dependence of X_1 on heat release rate and wind velocity and deduced a relationship considering that X_1 also is a function of Fr_{wind} and Q^*. While some scatter is recognized, and shown in Figure 11(a), (b), the X_1 can be given as follows.

- with floor (the surface of the fire source is set at the same level as the floor)

$$X_1 / D = 0.87\left(Fr_{wind}^{1/3}\cdot Q^{*2/3}\right)^{2/3} \tag{14}$$

- without floor

$$X_1 / D = 0.55\left(Fr_{wind}^{1/3}\cdot Q^{*2/3}\right)^{2/5} \tag{15}$$

In the case of "without floor" and with a relatively strong cross-wind, the flame shows the typical shape like overflowing from the burner and the main axis of the flame draws the different locus. Equation (15) is derived for lower wind velocities. Equations (14) and (15) show that the dependence of X_1 or Fr_{wind} and Q^* is similar both "with" and "without floor".

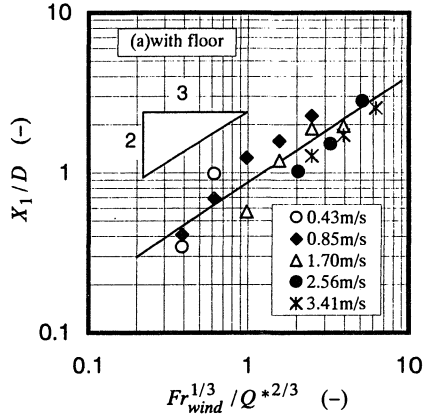

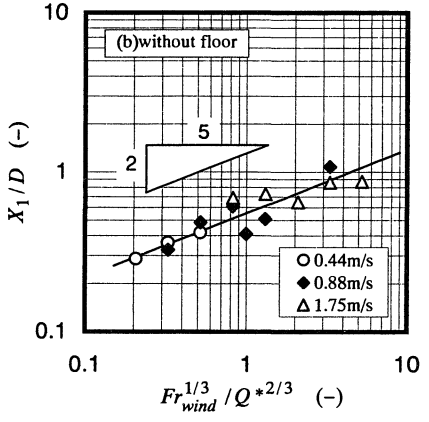

Figure 11 The dependence of X_1 on Fr_{wind} and Q^*.

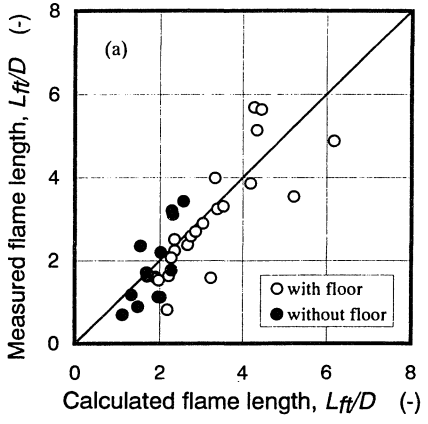

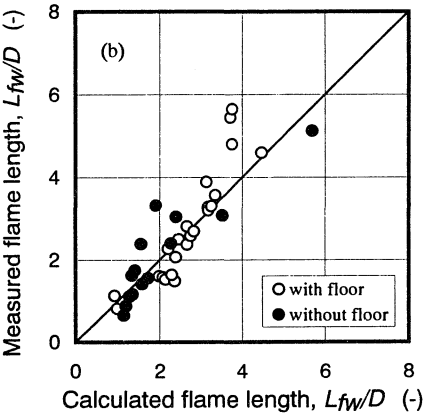

Figure 12 Comparison of calculated and measured flame length.
(a) L_{ft} is calculated with equation (16).
(b) L_{fw} is calculated with equation (17).

Flame length

The length along the flame axis can be calculated using the distance X_1, the apparent height and tilt angle θ_1 as follows.

$$L_{ft} \approx X_1 + H_f / \cos\theta_1 \tag{16}$$

Another relation between the length of the inclined flame, defined as the straight line from the centre of the burner surface to the extended flame tip, and the apparent flame length, is expressed as follows.

$$L_{fw} = \sqrt{H_f^2 + X_2^2} \tag{17}$$

The relation $X_2 = H_f \cdot \tan\theta_2$ between tilt angle and distance X_2 holds true. Figure 12(a), (b) shows a comparison between measured and calculated flame length from equations (16) and (17). It is obvious that the length of the inclined flame can be estimated using the apparent flame height and its tilt angle, regardless of the existence of the floor or not.

The following formula can be given after substituting the relation for flame tilt angle on θ_2, and the apparent flame height under the condition of "without floor", into equation (17).

$$\frac{L_{fw}}{D} = A\left(\frac{Fr_{wind}^{1/2}}{Q^{*1/6}}\right)^{1/2} + B\left(\frac{Q^{*3/2}}{Fr_{wind}^{3/2}}\right)^{1/2} \tag{18}$$

A similar formula can be obtained for "with floor". Equation (18) shows that the length of the inclined flame can not be simply represented as the product of Q^* and Fr_{wind}, but can be represented as the sum of two parts, with the dominant variable being either heat release rate or wind velocity.

The remaining issue is the width of the inclined flame. If we are able to develop a model for this, we would then be in a good position to estimate thermal intensity required at the design stage.

CONCLUSIONS

Dimensionless formulae for the apparent flame height of an inclined flame under the influence of cross-wind have been developed based on the dimensionless heat release rate and Froude number.

New formulae have been developed to predict the flame tilt angle, both with and without the presence of a floor. Each model is derived from the balance of mass fluxes of wind and hot current, combined with centerline properties of a fire plume.

The dependence of Fr_{wind} on the apparent flame height is different according to the local geometry in the vicinity of the fire source and the value of exponent varies from 2/3 to 1 according to the position of the fire source with respect to the ground.

The dependence of apparent flame height on Fr_{wind} and Q^* is similar both with and without the presence of a floor.

θ_1 and θ_2 are almost the same in the case of "without floor". Considering application of the model to confined floors, such as compartment fires, suggests that θ_1 becomes a more useful parameter than θ_2.

The inclined flame length can be estimated using models for the apparent flame height and tilt angle regardless of the existence of a floor or not.

ACKNOWLEDGEMENT

The authors would like to sincerely thank Mr. Hideaki Kuwana and Mr. Yoshiaki Arai, Kajima Technical Research Institute, for their assistance in the experiments.

REFERENCES

1) Sugawa,O., Satoh,H. and Oka,Y.: "Flame Height from Rectangular Fire Sources considering Mixing Factor", Int. Assoc. of Fire Safety and Science, Proceedings of the Third Int. Symposium on Fire Safety Science, pp.435-444, (1991)
2) Hasemi,Y. and Nishihata, M.: "Fuel Shape Effect on the Deterministic Properties of Turbulent Diffusion Flames", Int. Assoc. of Fire Safety and Science, Proceedings of the 2nd Int. Symposium on Fire Safety Science, pp.275-284, (1989)
3) Yokoi, S.: "On the Heights of Flames from Burning Cribs", Bull. Of the Fire Prevention Society of Japan, Vol.13, No.1, pp.22-27, (1963), in Japanese
4) Heskestad, G.: "Luminous Heights of Turbulent Diffusion Flames", Fire Safety Journal, Vol.5, pp.103-108, (1983)
5) Zukoski, E.E.: "Fluid Dynamic Aspects of Room Fires", IAFSS, Proceedings of the First Int. Symposium on Fire Safety Science, (1985)
6) Thomas, P.H.: "The Size of Flames from Natural Fires", 9th Int. Combustion Symposium, Comb. Inst., pp.844-859, (1963)
7) American Gas Association: "LNG Safety research Program", Report IS 3-1, (1974)
8) Pipkin, O. A. & Sliepcevich, C. M.: "Effect of Wind on Buoyant Diffusion Flames", ICE, Fundamentals, 3-2, p.147, (1964)
9) Quintiere, J.Q., Rinkinen, W. W. and Jones, W. W.: "The Effect of Room openings on Fire Plume Entrainment", Combustion Science and Technology, Vol.26, (1981)
10) Yumoto, T.: "Petrochemical Fire", Anzenkougaku, Vol.19, No.6, pp.360-367, (1980), in Japanese
11) Sugawa, O., Momita, D. and Takahashi, W.: "Flow Behavior of Ejected Fire Flame/Plume from an Opening Effected by External Side Wind", Int. Assoc. of Fire Safety and Science, Proceedings of the 5th Int. Symposium on Fire Safety Science, pp.249-260, (1997)
12) Saga, T.: "Study on Flame of Big Fire in Urban Area Under Strong Wind", Bulletin of Japan Association for Fire Science and Engineering, Vol.46, No.1-2, pp.1-12, (1997) , in Japanese
13) Drysdale, D.: An Introduction to FIRE DYNAMICS, p141, JOHN WILEY & SONS, (1986)
14) The SFPE Handbook of Fire Protection Engineering, 2nd Edition, Capture 3-12, National Fire Protection Association, (1995)
15) McCaffrey, B.J.: "Purely buoyant diffusion flames: some experimental results", NBSIR 79-1910, (1979)
16) Oka, Y., Kurioka, H., Satoh, H. and Sugawa, O.: "Theoretical Approach on Flame Tilt based on Apparent Flame Heights in Free Boundaries", Journal of Constr. Engng, AIJ, in printing (in Japanese)